Influence of longitudinal creepage and wheel inertia on short-pitch corrugation: a resonance-free mechanism to explain the roaring rail phenomenon

M Ciavarella[1]* and **J Barber**[2]
[1]CEMEC-DIASS, Politecnico di Bari, Bari Italy
[2]University of Michigan, MI, USA

The manuscript was received on 28 September 2007 and was accepted after revision for publication on 11 January 2008.

DOI: 10.1243/13506501JET373

Abstract: Short-pitch corrugation (30–80 mm in wavelength) in railways, despite being well known since the early days of the railways because of its criticality in producing damage, 'roaring rail' or 'howling wheel' noise, and indirectly rolling contact fatigue, is considered an enigmatic phenomenon. In fact, most available data seem to show a non-linearly increasing wavelength with speed, and an almost fixed wavelength, while most models based on system resonances predict a fixed frequency. More enigmatic still, many data points fall in a range of frequencies where there is no evident resonance in the wheel–railtrack system (the large gap between the low frequencies resonances from 50 to 300 Hz and the very high pinned–pinned mode resonant frequencies which correspond generally to 850–1100 Hz in railways. Yet the most common classifications of corrugation continue to associate corrugation to frequency-fixing mechanisms.

Johnson's early studies on the Hertz normal spring resonance suggest that plasticity-based repeats impact mechanism, or differential wear mechanism both seemed to be not appropriate to explain short-pitch corrugation. In particular, *longitudinal creepage* (obviously associated with braking or acceleration very common on uphill grades, near stations, but also in curves where profiles provide insufficient steering capability) seemed to act to suppress corrugation, rather than promoting it, as suggested in the model of Grassie and Johnson. Only a few, very comprehensive models that include all the relevant receptances consider the effect of wheel inertia: indeed, these models indicate many possible corrugation regimes and, in particular, point at lateral creepage mechanisms at the pinned–pinned resonant frequency as giving much larger growth than longitudinal creepage, so the possibility of a corrugation regime independent of wheelset or railtrack resonances has largely remained hidden, despite it being present in some results.

In this paper, a simple model that returns to a pure *longitudinal creepage* mechanism is suggested, showing that it is essential to include the rotational dynamics of the wheel in the system, similar to Grassie and Johnson's model. In particular, a simple full-stick Winkler-contact mechanics model can estimate the effect of transient contact mechanics. For typical inertias, the conditions are closer to the constant tangential load (which is the correct limit at zero speed anyway) and seem to explain the basic features of wear-induced instability in the existing experimental data. For larger inertias, which may also be possible for heavy wheelsets, the model predicts results closer to Grassie and Johnson's assumption of constant creepage, i.e. only a limited range of possible short-pitch corrugation. The model also suggests that although the growth of corrugation depends strongly on the amplification of the normal load, the wavelength of this mode of corrugation depends very little on the vertical resonances of the systems, so that it would

*Corresponding author: CEMEC-DIASS, Politecnico di Bari, Vle Gentile 182, Bari 70126, Italy. email: mciava@poliba.it

persist even in a model with no resonance altogether. It is possible that the exact frequency of this regime depends on the details of the contact geometry, here simplified using the Winkler model.

Finally, a reason why this mechanism of longitudinal creepage corrugation, despite perhaps giving 10–20 times apparently lower growth than lateral creepage, may indeed be the correct mechanism to interpret the classical data, is that longitudinal creepage can be 10 times higher than lateral (5 per cent instead of 0.5 per cent), and as corrugation growth is proportional to square of creepage, there is a factor 100 that largely compensates for this. There is still some progress to be made to obtain a reliable model to compare the various regimes, but clearly this regime should be considered when devising remedies to corrugation.

Keywords: corrugation, transient non-linear dynamic, perturbation, railways

1 INTRODUCTION

The application motivating this investigation is the study of 'corrugations' on the running surface caused by the action of the railways wheels, a phenomenon that has been observed throughout railway history, but not fully understood [**1**], particularly for short-pitch rail corrugation ('roaring rails') in the range of 20–80 mm wavelength, which seems to show a constant wavelength or a non-proportional increase of corrugation wavelength with increasing train speed. This common belief comes from the large amounts of data available in BR reports of 1911, in David Harrison's thesis [**2**], a figure from which is reproduced in the well-known paper by Grassie and Kalousek [**1**], and in the more recent paper by Bhaskar *et al.* [**3**], adapted here in Fig. 1.

In Harrison's data are particularly surprising because they seem to suggest an almost 'fixed wavelength', whereas the other results are linear in the given range, and do not start from the origin, suggesting perhaps some non-linear effect, or a threshold.

An important study was that of Grassie and Johnson [**4**], which despite using a simplified two-dimensional formulation and a 'Winkler' model for the contact problem, contained quite a few features and hence would be expected to give qualitatively reasonable predictions. However, unfortunately, one assumption was made that the authors of the current paper believe was critically incorrect: that longitudinal creepage would be constant, perhaps based on the more reasonable assumption that the large mass of the vehicle would make its speed constant. Grassie and Johnson found no mechanism for corrugation in the range of interest of Fig. 1 and actually suggested that this could be a mechanism for suppression of corrugation.

In many later studies, the models introduced many detailed improvements, although those modifying the assumption of constant longitudinal creepage generally include so many other effects that it is difficult to distinguish the relative roles of each, and the investigations are generally relative only to a special system under a certain range of conditions, so that the simplicity of the original Grassie and Johnson model to identify the main relevant features was lost.

For example, Frederick [**5**] introduced an elegant perturbation analysis via complex transfer functions, which makes it simple to check if the phase of the maximum dissipation would produce amplification of the original corrugation in the frequency range of interest. He studies both lateral and longitudinal creepage assuming for the wheel receptance the same concentrated mass model, similar to what is done in this paper, so the main difference between lateral and longitudinal creepage is the receptance of the rail (a pure damper longitudinally and a quite flexible structure laterally). The results show a dominant lateral creepage mechanism at pinned–pinned resonance, but also other possible regimes, *including one with longitudinal creepage not corresponding to a resonance (at about 750 Hz)* and only active above sleepers. It must be said that Frederick's model assumes a wear parameter that is not energy dissipation but more simply the Clayton creep-force one, and that it shows results only for a quite high velocity (40 or 60 m/s) and restricted to frequencies above 300 Hz, whereas here the entire range of velocities and frequencies is investigated. Also, the assumptions of saturated creep changes the relative effects of fluctuation of creepage and tangential force with respect to the more general condition at small creepage in the linear regime. A similar assumption is made here.

It must be also said that while many authors consider the wheelset resonances very narrow, perhaps removing them from the analysis, they are less cautious when dealing with the pinned–pinned resonance, which is also quite delicate to deal with – an error in the damping factor may easily change the amplitude response, and also the different pattern of corrugation along the sleeper bay is not always observed. Also, despite that the presence of the periodic structure does seem to trigger the corrugation mechanism [**5**], the pinned–pinned resonance frequency is not as frequently observed as the data in Fig. 1 suggest.

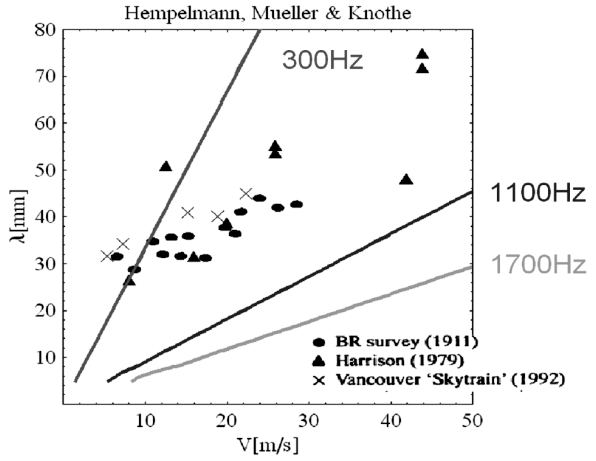

Fig. 1 Experimentally observed variation of corrugation wavelength with speed – adapted from Bhaskar et al [**3**]. Superposed are the constant frequencies of 300, 1100, and 1700 Hz, which some authors indicate as the resonances of the system which should justify corrugation

Tassilly and Vincents [**6**, **7**] further developed Frederick's model, applying it to the Paris metro system, and also adding the low-frequency resonances including the wheelset ones experimentally measured. In this case, there are few possibilities to attribute corrugation to one of these resonance frequencies, but ultimately they found predominantly transversal wear on the leading wheelset corresponding to its first bending mode (a lateral mechanism), and longitudinal wear on the rear one, related to the first torsional mode of the wheelset. Tassilly and Vincent's 'case 3, corrugation on a concrete track', however, does show a possible regime of corrugation independent of resonances. Elkins *et al.* [**8**] found that the 300 Hz (second) torsional resonance for the wheelset may be responsible for some types of corrugation.

The effect of discrete sleepers is also included by Hempelmann [**9**] (see also reference [**10**]), who use a linearization over the full non-linear model for creepage law, and return to the energy dissipation parameter. They also include sophisticated numerical treatments developed to deal with transient contact effects by Gross–Thebing [**11**]. Unfortunately, they neglect longitudinal creepage, so have receptances only in the lateral direction. Similarly to Frederick, they find corrugation growth in almost the entire range from 0 to 2000 Hz (except at the pinned–pinned resonance) at midspan, whereas above sleepers they found a regime around the 350 Hz (which was 500–600 Hz in Frederick's study) and more importantly at the pinned–pinned resonance frequencies and higher where the magnitude is much higher than the other regime. Only the presence of the pinned–pinned regime has generally been considered as Hempelmann's results*, and not the underlying mechanism for growth clearly not associated to resonances of the system – which may perhaps be the only left in a system with continuously laid track, or when longitudinal creepage is considered instead of lateral, especially as longitudinal creepage is generally much larger than the lateral (see in particular the illuminating discussion which is a part of the Hempelmann and Knothe 1996 paper by Frederick). Moreover, even if is assumed that growth initiates at the sleepers, probably the process continues through a continuous range of wavelengths depending on position. The large collection of data in Fig. 1 could not be explained by the pinned–pinned range which for practical speeds is concentrated in the 20–30 mm range, but could also be the result of some averaging. However, it is very likely that longitudinal creepage plays a role; for example, Vancouver SkyTrain's short-pitch corrugation was largely unaffected by sleeper spacing [**3**]. So why could Grassie and Johnson's model not find such a mechanism?

In principle, Muller [**12**, **13**] extends the Hempelmann model. However, he omits the dynamic motion of wheel and tends to find agreement with Hempelmann's results, suggesting mainly pinned–pinned resonance corrugation, with perhaps other secondary regimes at 300 and 1700 Hz, as indicated in Fig. 1 with the three lines clearly not sufficient to explain the experimental values.

The conclusion of Grassie and Johnson [**4**] that longitudinal creepage would more likely suppress corrugation than promote it in the short-pitch range was never really reassessed, as Hempelmann had neglected longitudinal creepage, and although some authors do include wheelset receptances (Frederick, Tassilly and Vincents, etc.) and seem to indicate longitudinal creepage mechanisms, it is a little unclear if these are necessarily to be associated to resonances of the system or not.

Bhaskar *et al.* [**3**] also looked at the problem, but from a different perspective of *spin-creepage* corrugations as a result of closely conformal wheel and rail profiles. They quite honestly do not seem happy with the prediction of their model, which however neglects wheelset receptances (and hence all inertia effects) and otherwise could have been compared with that of Hempelmann [**9**], and Hempelmann and Knothe [**10**].

In the present paper, returning to the simple case of *longitudinal-creepage* and reconsidering the analysis of Grassie and Johnson [**4**], the assumption of

*A second regime is suggested by Hempelmann and Knothe between 200 and 450 Hz regime for systems with high pad-stiffness. This must be the regime considered in Hempelmann's original thesis [**9**] whose chapter 7 rather points at corrugation being highest in the regimes of 400 and 1450 Hz.*

constant longitudinal creepage is substituted by, the rotational inertia of the wheel. It is demonstrated that this simple modification is sufficient to make predictions that are quite close to experimental observations. The attempts of more sophisticated models should therefore perhaps introduce longitudinal creepage, unless there is clear evidence of its absence, and consequently of wheel inertia and rotational dynamics.

2 THE MODEL

A simple model very close to that of Grassie and Johnson [**4**] is attempted here, but including wheel inertia and using a linear perturbation approach. The Winkler or wire-brush model assumes that the tangential tractions are proportional to the displacements

$$q = k_q u_x \tag{1}$$

where k_q is a Winkler modulus which must be chosen by some best-fit criterion. This leads to a considerable simplification, since all coupling effects leading to integral equations are eliminated. All other aspects of the model are simplified as much as possible, since the paper seeks merely to demonstrate that the effect of wheel inertia is critical to the generation of a regime of corrugation – which has so far has escaped attention – and which here is found only with qualitatively realistic predictions. In particular, attention is restricted to two dimensions and the model used, taken from the literature and representative only of an intercity track, describes the rail dynamics. Clearly these approximations are very restrictive and exclude many effects, such as the pinned–pinned resonance due to sleeper spacing, interaction of adjacent wheelsets, three-dimensional (lateral) effects: all these effects may be more able to generate alternative regimes of corrugations. A quantitatively accurate model which could assess the relative importance of all these modes has so far not been produced. Hence, the present model is introduced to produce evidence of the regime of corrugation which depends on only a few geometrical and one loading parameter (mean normal load), making the qualitative effect of these parameters easy to assess.

It is assumed that the vehicle is moving to the left at constant speed V, so that the wheel is rotating counter-clockwise at some speed Ω. A rigid-body velocity V is superposed to the right, bringing the centre of the wheel to rest, and causing the rail to move at speed V to the right. Assuming that the vehicle is braking, the friction force on the wheel opposes the direction of motion V and hence is to the right, and the braking torque B opposes the direction of rotation, as shown in Fig. 2. This figure also shows the

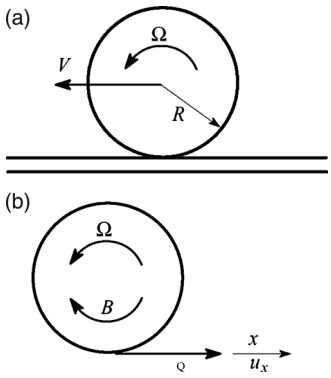

Fig. 2 The wheel-rail contact point and coordinate system

sign convention for the coordinate x and for the elastic displacement u_x of a point on the wheel in the contact zone.

If there was no elastic deformation, the velocity of a point on the wheel in the contact region in the x-direction would be ΩR. However, the steady-state tensile strain $\partial u_x/\partial x$ and the elastic displacement variation in time add so that the rightward velocity of a point on the wheel is

$$v_x = \left(1 + \frac{\partial u_x}{\partial x}\right)\Omega R + \frac{\partial u_x}{\partial t} \tag{2}$$

All the elastic deformation in concentrated in the wheel, which means that an equivalent modulus for the wheel is used treating the rail (or the surface) as rigid. In that case, points on the rail move at constant speed V and a slip velocity

$$\dot{s}_x = V - \Omega R - V\frac{\partial u_x}{\partial x} - \frac{\partial u_x}{\partial t} \tag{3}$$

can be defined in the direction that points on the rail, slipping to the right relative to the wheel. Further, suppose that the coefficient of friction is sufficiently high to prevent slip occuring anywhere: $\dot{s}_x = 0$ and hence

$$V\frac{\partial u_x}{\partial x} + \frac{\partial u_x}{\partial t} = V - \Omega(t)R \tag{4}$$

The wheel may not spin at a constant rate due to rotational dynamics and it is assumed that $\Omega(t)$ is a known function and, in fact, it will typically have the form

$$\Omega(t) = \Omega_0 + \Omega_1 \exp(\imath\omega t) \tag{5}$$

The general solution of equation (4) is

$$u_x(x,t) = f(x - Vt) + Vt - \Omega_0 Rt + \frac{\imath\Omega_1 R}{\omega}\exp(\imath\omega t) \tag{6}$$

where f is any arbitrary function of $(x - Vt)$. This function is determined in practice by the conditions at the

leading edge of the contact, where the instantaneous state of the surface is 'locked-in' to a state of stick.

For the boundary condition, it is assumed that the shear traction at the leading edge is zero, i.e. $q_x(-a)=0$, and hence in view of the Winkler foundation

$$u_x(-a,t)=0 \tag{7}$$

at all times t.

Notice that in a full three-dimensional elasticity solution, there will be tensile strains ahead of the contact and hence the elastic displacement at the leading edge will be non-zero. However, the Winkler assumption is the basis of the 'simplified' theory of Kalker [**14**] and also of his numerical algorithm 'FASTSIM' [**15**] and has been shown to agree quite well with the more exact theory in other respects.

In the steady state, there is no dependence on t and $\Omega_1=0$. Then

$$f(-a-Vt)+Vt-\Omega_0 Rt=0 \tag{8}$$

Writing $\eta=-(a+Vt);\ t=-(a+\eta)/V$, then $f(\eta)=(V-\Omega_0 R)(a+\eta)/V$, and for the displacement u_x, the linearly varying term from zero is recovered at the leading edge of the Carter [**16**] classical solution

$$\begin{aligned} u_x &= \frac{(V-\Omega_0 R)(a+x-Vt)}{V}+Vt-\Omega_0 Rt \\ &= \xi_0(a+x) \end{aligned} \tag{9}$$

see Barber [**17**], where a steady-state creepage ratio is introduced

$$\xi_0=\left(1-\frac{\Omega_0 R}{V}\right) \tag{10}$$

Since the equations are linear, the oscillatory solution can be written as the sum of the steady-state solution and an oscillatory term which has to satisfy the equation

$$u_x^{\omega}=f^{\omega}(x-Vt)+\frac{\imath\Omega_1 R}{\omega}\exp(\imath\omega t) \tag{11}$$

with boundary condition $u_x^{\omega}(-a,t)=0$ at all times t. Applying the boundary condition, the complete transient solution is then

$$\begin{aligned} u_x &= \xi_0(a+x)+\frac{\imath\Omega_1 R}{\omega}\exp(\imath\omega t) \\ &\quad\times\left[\exp\left(-\frac{\imath\omega(a+x)}{V}\right)-1\right] \end{aligned} \tag{12}$$

It is easily verified that this expression satisfies the original governing equation (4) and the boundary condition (7) at all times t. The displacement must of course be a real quantity, and so the real part of this has to be extracted to describe the physics of the problem.

The time-varying tangential force $Q(t)$ is given by

$$Q(t)=\int_{-a}^{a}q_x(x)\mathrm{d}x=k_q\int_{-a}^{a}u_x(x)\mathrm{d}x \tag{13}$$

from equation (1) and substituting for u_x from equation (12) and performing the integration, $Q(t)=Q_0+Q_1\exp(\imath\omega t)$, where

$$\begin{aligned} Q_0 &= 2k_q\xi_0 a^2\ ;\ \ Q_1=\frac{2k_q\Omega_1 Ra}{\omega}\left\{\frac{V}{2\omega a}\right. \\ &\quad\left.\times\left[1-\exp\left(-\frac{2\imath\omega a}{V}\right)\right]-\imath\right\} \end{aligned} \tag{14}$$

2.1 Effect of varying normal force

So far, only oscillations in tangential load and angular velocity have been considered, but the driving term of the present problem is an oscillation of the normal force in time, due to some existing corrugation

$$\Delta\exp(\imath\omega t)$$

where $\omega=2\pi f=2\pi V/\lambda$ and λ is the wavelength of the corrugation. In fact, the objective of the analysis is to determine which if any wavelengths lead to oscillations such that the resulting wear occurs at the troughs of the corrugation and hence amplification of an initial perturbation.

The corresponding oscillation in the normal contact force $P(t)$ will cause the semi-length of the contact a to oscillate, so

$$a(t)=a_0+a_1\exp(\imath\omega t) \tag{15}$$

Equation (6) remains unchanged when a is non-constant, but the boundary condition (7) becomes

$$u_x(-a(t),t)=0 \tag{16}$$

giving

$$\begin{aligned} &f(-a_0-a_1\exp(\imath\omega t)-Vt)+Vt \\ &\quad-\Omega_0 Rt+\frac{\imath\Omega_1 R}{\omega}\exp(\imath\omega t)=0 \end{aligned} \tag{17}$$

Since $a_1\ll a_0$, the first term is expanded as

$$\begin{aligned} &f(-a_0-a_1\exp(\imath\omega t)-Vt) \\ &\quad=f(-a_0-Vt)-f'(-a_0-Vt)a_1\exp(\imath\omega t) \end{aligned} \tag{18}$$

and the complete function as the form $f(\eta)=f_0(\eta)+f_1(\eta)$, where $f_1\ll f_0$, and $f_0(\eta)=(1-\Omega_0 R/V)(a_0+\eta)$,

and f' can be replaced by $f_0' = (1 - \Omega_0 R/V)$. Then, writing $\eta = -(a_0 + Vt)$; $t = -(a_0 + \eta)/V$

$$f(\eta) - a_1 f'(\eta)\exp(\imath\omega t) - \left(1 - \frac{\Omega_0 R}{V}\right)(a_0 + \eta) + \frac{\imath\Omega_1 R}{\omega}\exp(\imath\omega t) = 0 \quad (19)$$

and hence

$$f_1(\eta) = a_1\left(1 - \frac{\Omega_0 R}{V}\right)\exp\left(-\frac{\imath\omega(a_0+\eta)}{V}\right) - \frac{\imath\Omega_1 R}{\omega}\exp\left(-\frac{\imath\omega(a_0+\eta)}{V}\right) \quad (20)$$

The displacement u_x is then recovered from equation (6) as

$$u_x = \left(1 - \frac{\Omega_0 R}{V}\right)(a_0 + x) + \frac{\imath\Omega_1 R}{\omega} \times \left[1 - \exp\left(-\frac{\imath\omega(a_0+x)}{V}\right)\right]\exp(\imath\omega t) + a_1\left(1 - \frac{\Omega_0 R}{V}\right)\exp\left(-\frac{\imath\omega(a_0+x)}{V}\right)\exp(\imath\omega t) \quad (21)$$

2.2 Tangential load and dissipation

To obtain the tangential load for the general case just solved of varying angular speed and normal load, the following has to be calculated

$$\int_{-a}^{a} u_x(x)\mathrm{d}x \approx \int_{-(a_0+a_1\exp(\imath\omega t))}^{(a_0+a_1\exp(\imath\omega t))}\left(1 - \frac{\Omega_0 R}{V}\right)(a_0 + x)\,\mathrm{d}x + \exp(\imath\omega t)\int_{-a_0}^{a_0}\left[\frac{\imath\Omega_1 R}{\omega}\left[1 - \exp\left(-\frac{\imath\omega(a_0+x)}{V}\right)\right] + a_1\left(1 - \frac{\Omega_0 R}{V}\right)\exp\left(-\frac{\imath\omega(a_0+x)}{V}\right)\right]\mathrm{d}x$$

where only first-order terms in the perturbation have been included. The first integral is trivial, and the term involving Ω_1 is identical with that for constant a and contributes a term

$$\frac{2\Omega_1 R a_0}{\omega}\left\{\frac{V}{2\omega a_0}\left[1 - \exp\left(-\frac{2\imath\omega a_0}{V}\right)\right] - \imath\right\}\exp(\imath\omega t)$$

from equation (14). Finally, for the term involving a_1

$$\int_{-a_0}^{a_0}\exp\left(-\frac{\imath\omega(a_0+x)}{V}\right)\mathrm{d}x = -\frac{V}{\imath\omega}\left[\exp\left(-\frac{2\imath\omega a_0}{V}\right) - 1\right] \quad (22)$$

The dissipation rate under full stick conditions, is given by the release of the energy at the trailing edge, which can be found from

$$D(t) = \frac{1}{2}Vk_q[u_x(a(t))]^2 = \frac{1}{2}Vk_q[u_x(a_0 + a_1\exp(\imath\omega t))]^2$$

where, substituting equation (15) into equation (21) and dropping second-order terms gives

$$u_x(a(t)) = 2\xi_0 a_0 + \xi_0 a_1\exp(\imath\omega t) + \left[\frac{\imath\Omega_1 R}{\omega} + \left(\xi_0 a_1 - \frac{\imath\Omega_1 R}{\omega}\right)\exp\left(-\frac{2\imath\omega a_0}{V} \times \left(1 + \frac{a_1}{2a_0}\exp\imath\omega t\right)\right)\right]\exp(\imath\omega t) \quad (23)$$

The dissipation rate can therefore be written as $D(t) = D_0 + D_1\exp(\imath\omega t)$, and collecting results for Q and D

$$Q_0 = 2k_q\xi_0 a_0^2 \quad D_0 = V\xi_0 Q_0 \quad (24)$$

and

$$Q_1 = 2\xi_0 k_q a_0 a_1\left\{1 - \frac{\imath}{\zeta}\left(1 - \exp(-\imath\zeta)\right)\right\} - \Omega_1\frac{4a_0^2 R k_q}{V}\frac{1}{\zeta}\left\{\frac{1}{\zeta}\left(1 - \exp(-\imath\zeta)\right) - \imath\right\} \quad (25)$$

$$D_1 = 4k_q V\xi_0^2 a_0 a_1\frac{\left(1 + \exp(-\imath\zeta)\right)}{2} + 4k_q V\xi_0 a_0^2\frac{2i\Omega_1 R}{V}\frac{\left(1 - \exp(-\imath\zeta)\right)}{2\zeta} \quad (26)$$

where the parameter is defined as

$$\zeta = \frac{2\omega a_0}{V} = \frac{4\pi a_0}{\lambda} \quad (27)$$

which represents the extent of the initial corrugation (in radians) present in the contact area at any given time.

The term a_1 can be related to the perturbation in normal load P. Using the Hertzian relation

$$a = 2\sqrt{\frac{PR}{\pi E^*}} \quad (28)$$

and perturbing about the mean load P_0, the following is obtained

$$a_1 = \frac{\partial a}{\partial P}P_1 = P_1\sqrt{\frac{R}{\pi P_0 E^*}} = \frac{P_1 a_0}{2P_0} \quad (29)$$

3 OBSERVATION AND 'TUNING' OF THE SOLUTION

Equations (25) and (29) define the dynamic relationship between the perturbations Q_1, P_1, and Ω_1

in tangential force, normal force, and rotational speed, respectively, and hence define the frequency-dependent receptance of the contact process under the Winkler spring assumption for tangential contact. Most authors (except those using the Gross-Thebing numerical technique) obtain an expression for this receptance by either assuming arbitrary simplification of the contact with elastic springs, or by simply perturbing the appropriate steady-state creep relation about the mean state, which is equivalent to assuming that the steady-state relation applies even under transient conditions. This assumption is reasonable in the low frequency limit ($\zeta \to 0$) and indeed might be expected to give reasonable results for moderate values of ζ, since Kalker showed that transient effects in rolling contact become essentially negligible after a rolling distance equal to the contact width, but unfortunately, short-pitch corrugation does not fall into the range of 'moderate values of ζ'. Appropriate values of the parameters are $\lambda = 20$–80 mm and $a_0 = 3$–5 mm, giving values of ζ in the range $0.4 < \zeta < 3$! Since the zeroth-order approximation is equivalent (in terms of tangential load) to a dashpot, some authors (e.g. [**3**]) have attempted to improve this zeroth-order approximation by adding a contact spring in series with a dashpot with parameters obtained from a combination of the Carter and Mindlin solutions. However, this technique only fits the tangential load, and nothing is said about the energy dissipation – the coefficients are not trivially obtained from those of tangential load, as it will be clearer in the following.

Since the perturbed Carter theory is exact in the limit $\zeta \to 0$, it is convenient to choose the value for the tangential stiffness k_q in the present Winkler model such that the two theories agree in the limit. The Carter solution gives the relation

$$\xi = 1 - \frac{\Omega R}{V} = \frac{fa}{R}\left(1 - \sqrt{1 - \frac{Q}{fP}}\right) \tag{30}$$

and in the 'full stick' limit as $f \to \infty$, this reduces to

$$Q = \sqrt{PR\pi E^*}\left(1 - \frac{\Omega R}{V}\right) \tag{31}$$

where equation(28) to substitutes for the contact semi-width a. Perturbing this expression with respect to Ω gives

$$Q_1 = -\frac{\Omega_1 R}{V}\sqrt{P_0 R\pi E^*} \tag{32}$$

This is compared with the second of equation (14), which in the limit $\omega \to 0$ tends to

$$Q_1 = -\frac{8k_q P_0 R^2}{\pi E^* V} \tag{33}$$

from which it is deduced that the two models will predict the same tangential receptance in the low frequency limit if

$$k_q = \frac{\pi E^*}{8}\sqrt{\frac{\pi E^*}{P_0 R}} = \frac{\pi E^*}{4a_0} \tag{34}$$

Using this result, equations (25) and (26) can be written in the form

$$Q_1 = C_P P_1 + C_\Omega \Omega_1, \quad D_1 = D_P P_1 + D_\Omega \Omega_1 \tag{35}$$

where

$$C_P(\zeta) = \frac{\xi_0}{2}\sqrt{\frac{\pi E^* R}{P_0}}\left[1 - \frac{\imath}{\zeta}\left[1 - \exp\left(-\imath\zeta\right)\right]\right] \tag{36}$$

$$C_\Omega(\zeta) = -\frac{2}{V\zeta}\sqrt{\pi E^* P_0 R^3}\left\{\frac{1}{\zeta}\left[1 - \exp\left(-\imath\zeta\right)\right] - \imath\right\} \tag{37}$$

$$D_P(\zeta) = \frac{V\xi_0^2}{2}\sqrt{\frac{\pi E^* R}{P_0}}\left(1 + \exp\left(-\imath\zeta\right)\right) \tag{38}$$

$$D_\Omega(\zeta) = 2\imath\xi_0\sqrt{\pi E^* P_0 R^3}\frac{\left(1 - \exp\left(-\imath\zeta\right)\right)}{\zeta} \tag{39}$$

4 COUPLING WITH THE DYNAMICS

To complete the analysis, the rotational equation of motion is written for the wheelset, which is simplified by omitting stiffness and damping, giving

$$I_\mathrm{w}\frac{d\Omega}{\mathrm{d}t} = (Q - Q_0)R \tag{40}$$

where I_w is the inertia of the wheel. It follows that the oscillatory terms are related by the equation

$$i\omega I_\mathrm{w}\Omega_1 = Q_1 R \tag{41}$$

and substituting for Ω_1 from equation (41) into the first equation (35) gives

$$Q_1 = C_P(\zeta)P_1 + C_\Omega(\zeta)\frac{Q_1 R}{i\omega I} \tag{42}$$

Solving for Q_1, and using $\zeta = 2\omega a_0/V$, the tangential load oscillatory term can be written in the perturbation as a function of the oscillatory term in normal load only

$$Q_1 = \frac{C_P(\zeta)}{1 - (C_\Omega(\zeta)/\zeta)(2Ra_0/iI_\mathrm{w}V)}P_1 \tag{43}$$

For dissipation, substituting Ω_1 from equation (41) into the second equation (35) gives

$$D_1 = D_P(\zeta)P_1 + D_\Omega(\zeta)\frac{Q_1 R}{i\omega I_\mathrm{w}} \tag{44}$$

which can be expressed in terms of P_1 using equation (43).

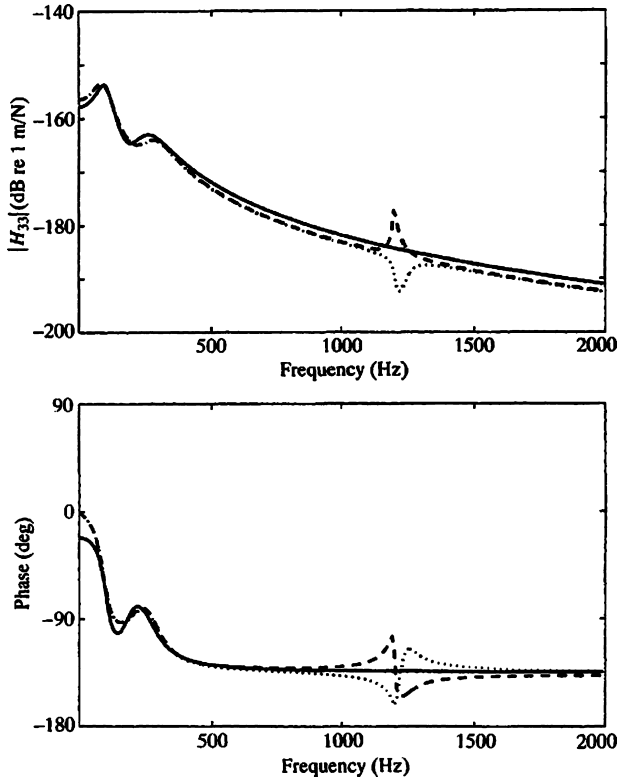

Fig. 3 The vertical receptance adapted from Bhaskar *et al.* [**3**]. The dotted lines are from a richer model including the pinned–pinned resonance, not used in the present study

The limit of constant creepage assumed by Grassie and Johnson [**4**] corresponds to the case where the wheel inertia is very large, or more precisely where the dimensionless parameter

$$\mathcal{I} \equiv \frac{I_w V^2}{P_0 R^3} \to \infty$$

At the other extreme, the assumption of constant tangential load, as in Grassie and Edwards [**18**] and Meehan *et al.* [**19**], corresponds to the case $\mathcal{I} \to 0$.

For the normal dynamics (i.e. the relation between the complex amplitude of the perturbation in normal force P_1 and the initial corrugation Δ), the rail vertical receptance of Bhaskar *et al.* [**3**] is used, which represents a typical BR rail with an equivalent continuous support (results from discrete support from Ripke's calculations for Intercity track having similar parameters are shown for comparison mid-way between sleepers (dashed lines) and at a sleeper (dotted lines).

5 RESULTS

The complex dissipation D_1, depends on only two parameters: (i) the inertia of the wheel and (ii) the steady normal load P_0. For the latter, $P_0 = 50$ kN is used

Table 1 The data of Nielsen *et al.* [[**20**]]

Train	M_{unspr} (kg)	R (m)	polarI (kg m^2)	1/2 M R^2	β	Axle load (tonnes)
X2 powered wheelset	1915	0.55	250	290	0.86	18.5
X2 trailer wheelset	1390	0.44	70	134	0.52	12.5

and for the inertia

$$I = \frac{\beta}{2} M_w R^2$$

where β is a factor ranging in general from 0.5 to 0.8, since the mass of the wheelset is concentrated near the centre. Nielsen *et al.* [**20**] for example report the data in Table 1. Considering that for a single wheel one half of the inertia values in the the polar inertia of the entire wheelset is taken, the values seem to range from 35 to 125 kg m^2, whereas most systems may have somewhat lower values with mass of the wheel around 350 kg and hence inertia in the range 18–30 kg m^2.

For completeness and simplicity, consider $\beta = 0.75$ and two cases:

(a) the mass of the wheel 350 kg, with a normal load of 50 kN, as a realistic value for a standard systems (where most data on Fig. 1 would likely fall), and compared with the limit case;
(b) the powered X2 wheelset using 1000 kg of mass as representative of a heavy loaded case with higher values $P_0 = 90$ kN.

To model the dynamic normal load, the rail receptance (from Bhaskar's model – see Fig. 3), the wheel receptance, and that of the Hertzian contact spring have to be added. Finally, the correction on the phase of dissipation resulting from the fact that the highest dissipation occurs at the rear of the contact, and not at its centrepoint, is added. Results for steady-state longitudinal creepage are shown, but the value of the creepage, as well as the friction coefficient and other parameters (like the vertical load) only affect the rate of growth of the corrugation, not the preferred (most rapidly growing) wavelength. Hence, the beauty of the qualitative model proposed here is that all these parameters need not to be fixed.

The dominant wavelength is expected to be that for which the predicted wear rate at the troughs is a maximum and this corresponds to the case where the dissipation function D_1 has the maximum negative real part. The following figures show 10 equally spaced contour levels from zero to the maximum negative real part of dissipation function, as a function of speed and wavelength of corrugation. Coloured lines show constant frequency 300, 1000, and 1700 Hz for reference, also equal to the lines in Fig. 1, and the experimental data points from Fig. 1 are also included. The bold lines

show the wavelengths corresponding to the maximum negative real part of D_1 as a function of speed V.

Figure 4 shows the result of the standard case A, showing considerable agreement with experiments. Most of the experimental data points fall in a region of the possible growth (where the real part of D_1 is negative), and most data also seem to concentrate around the bold line of the maxima, which at low speeds does some zigzaging because the dissipation function is first relatively flat, then follows almost a constant frequency (around 400 Hz), and then jumps to another regime (of high speed and high frequency, crossing the 1700 Hz line).

Figure 5, by contrast, shows no significant evidence of agreement between predictions and experimental data.

5.1 Wheel inertia and the two limit assumptions

To compare with the previous theories of Grassie and Johnson [**4**], Grassie and Edwards [**18**] and Meehan *et al.* [**19**], the limiting cases for constant tangential load (Fig. 6) and constant creep rate (Fig. 7) are presented by choosing the dimensionless wheel inertia $\mathcal{I}$ to be either very small or very large.

The predictions differ substantially from the experimental data in both cases. The results for constant tangential load show some modest qualitative agreement, although corrugation is predicted at much higher apparent frequency, whereas no substantive agreement with data is seen for large inertia, as was already apparent from Fig. 5.

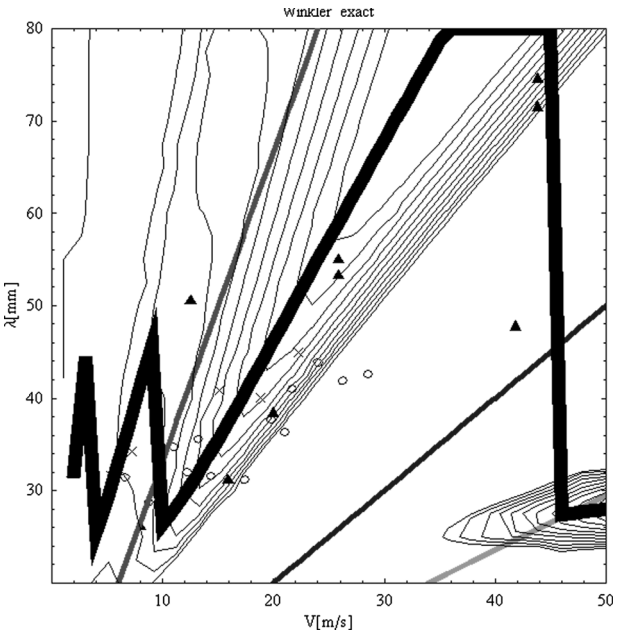

Fig. 4 The results for case A problem in this paper

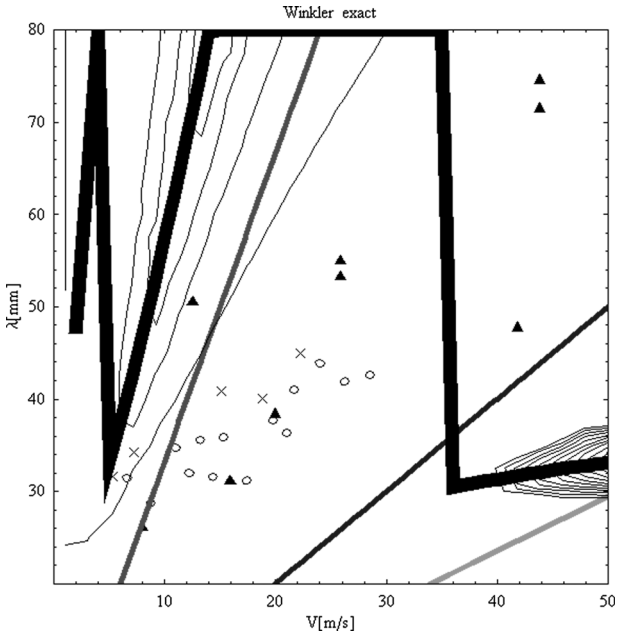

Fig. 5 The results for case B – high inertia

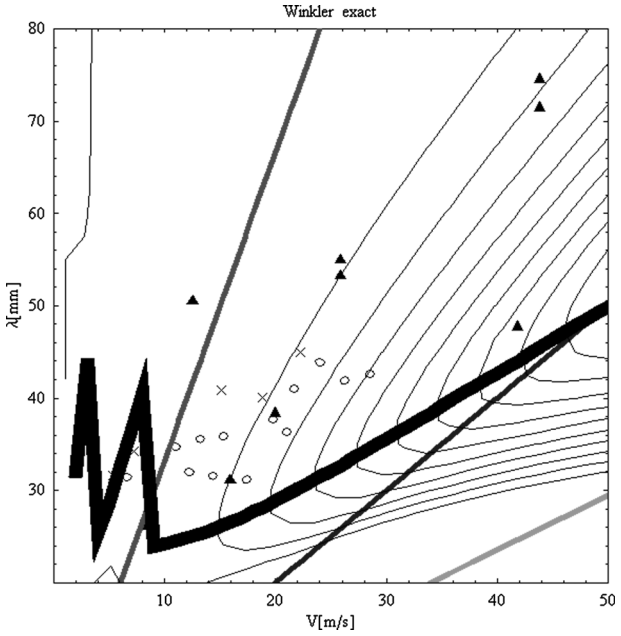

Fig. 6 The results for case A under the assumption of constant tangential load

6 DISCUSSION

The results in the current paper cannot pretend to answer all the questions raised by corrugation mechanisms and experimental data around, including different railways and metro systems. The Vancouver Skytrain of which the data on the vertical receptance was used was continuously supported on a concrete base with a 25 mm continuous rubber pad under

the rail. Periodic clips held the rails in place. Here, pinned–pinned resonance could not be even suggested as a mechanism, yet the data in Fig. 1 are surprisingly 'similar' to the data on BR 1911 report with probably wooden sleepers, so again pinned–pinned resonance had to be of marginal importance here. The results suggest that a possible mechanism is longitudinal creepage. That Grassie and Johnson [**4**] found no mechanism for short-pitch corrugation using longitudinal creepage was as shown here, due to the assumption of infinite wheel inertia. This erroneous conclusion, however, did not stop Frederick from making an excellent contribution just 1 year later (1986), which included the wheel inertia in both lateral and longitudinal directions. However, the fact that he found a longitudinal creepage mechanism very similar to what has been found here has largely remained obscure, since his regime (at 750 Hz) showed a growth factor 20 times lower than the lateral creepage mechanism, it was only explained for above sleepers, whereas for midsleepers there was again no mechanism (notice also that no pinned–pinned resonance regime was found for longitudinal creepage neither at above sleepers nor midspan by Frederick). There are many details of Frederick model which do not permit a rapid evaluation, but clearly this factor 20 could largely be outweighed by the fact that in the linear regime, growth is proportional to the square of creepage, and longitudinal creepage can be perhaps be 10 times higher than lateral (5 per cent instead of 0.5 per cent). Therefore, here there is a factor 100 which largely compensates, and suggests again longitudinal creepage associated with no resonance may be indeed

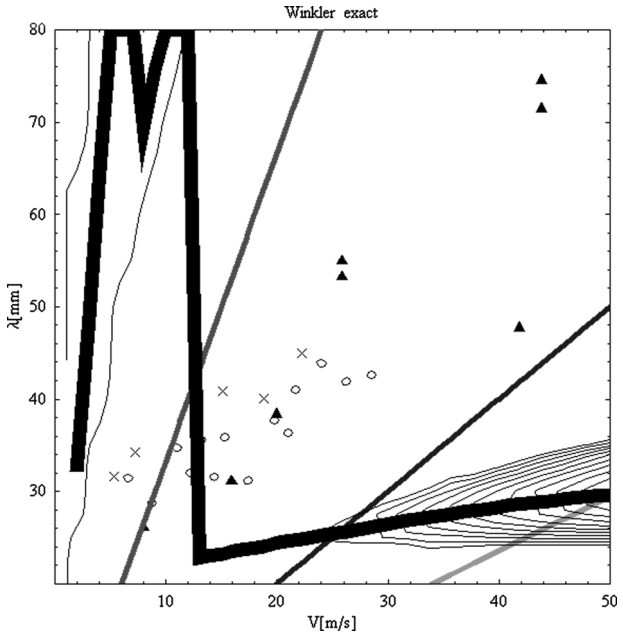

Fig. 7 The results for for case A under the assumption of constant longitudinal creepage

the correct mechanism to interpret the classical data, as first impressions from the comparison seems to indicate.

Later studies by the Berlin group improved many aspects of the Frederick model, but in one respect they took a step backwards, in that they did not generally include longitudinal dynamics – whether this is because of the original Grassie and Johnson [**4**] finding, or the Frederick result, or neither, is a matter of speculation. Hempelmann [**9**] finds highest growth for lateral creepage at sleepers at pinned–pinned resonance, but no growth midspan at this frequency where he finds much lesser growth at 'no-characteristic' frequency.

BR was very active in this area of research and did many surveys after 1911, which left the impression that corrugation on BR was insignificant until the introduction of continously welded rail and concrete sleepers in 1966. The reason for this is still unclear. More investigation is still required to solve this difficult problem.

7 CONCLUSIONS

A simple two-dimensional model has been developed using a full-stick Winkler (wire brush) approximation for the tangential contact problem with a modulus chosen to fit the classical Carter solution in the steady state. Starting from a given small sinusoidal corrugation profile and realistic values for the vertical receptance of the rail, the tangential dynamics of the problem were modelled, including the effect of finite wheelset rotational inertia. Corrugation is predicted to grow when the rate of energy dissipation is positive at the troughs of the original corrugation and the preferred wavelength is predicted to be that whose dissipation rate at this location is a maximum.

Corrugation from longitudinal creepage is found to be qualitatively explained in the range of realistic parameter values and the predicted wavelengths are reasonably close to those observed experimentally as a function of train speed. By considering the limits of large and small wheelset inertia, it was demonstrated that the constant creep rate assumption of Grassie and Johnson [**4**] or Bhaskar *et al.* [**3**] could not explain corrugation; reasons for more recent successful attempts assuming constant tangential load have also been given.

It can be concluded that it is critical to include the rotational dynamics of the wheelset in analyses of corrugation, and this confirms results found but neglected in previous models (Frederick, Hempelmann, Tassilly and Vincent), which include the wheel inertia, in that a regime not driven by a resonance of the system (neither of the track or the wheelset) is found possible. Despite that longitudinal

creepage seems to show less growth than lateral creepage mechanism, the much larger values for longitudinal creepage could largely compensate for this effect, and the much better agreement with the experimental data of the longitudinal creepage mechanism indicated here than to the 'pinned–pinned' resonance lateral mechanism is a strong indication that some conclusions in the literature should be revised. A more accurate quantitative model would require a more realistic contact model, including the effects of partial slip, and this is the subject of an ongoing investigation.

Additionally, the conclusions about pinned–pinned resonances coming only from numerical models may partly be erroneous due to difficulties of modelling of the resonances themselves (particularly, damping factors, strongly influencing amplitude response), parametric resonance effects, and perhaps the most urgent requirement is for more precise experimental data to complete, compare and distinguish the collection of Fig. 1.

ACKNOWLEDGEMENTS

The authors thank K. L. Johnson and J. Woodhouse from Cambridge University and S. L. Grassie, for helpful discussions regarding the present model. Also, Luciano Afferrante for help in the ongoing development of this model.

REFERENCES

1 **Grassie, S. L.** and **Kalousek, J.** Rail corrugations. Characteristics, causes and treatments. *Proc. Instn Mech. Engrs, Part F: J. Rail and Rapid Transit*, 1993, **207**, 57–68.

2 **Harrison, D.** *Corrugation of railways*. PhD Thesis, Cambridge University, UK, 1979.

3 **Bhaskar, A., Johnson, K L., Wood, G. D.,** and **Woodhouse, J.** Wheel-rail dynamics with closely conformal contact. Part 1: dynamic modelling and stability analysis. *Proc. Instn Mech. Engrs, Part F: J. Rail and Rapid Transit*, 1997, **211**, 11–26.

4 **Grassie, S. L.** and **Johnson, K. L.** Periodic microslip between a rolling wheel and a corrugated rail. *Wear*, 1985, **101**, 291–305.

5 **Frederick, C. O.** A rail corrugation theory. In Proceedings of the 2nd International Conference on *Contact mechanics of rail–wheel systems*, University of Rhode Island, 1986, pp. 181–211 (University of Waterloo Press, Waterloo, Ontario, Canada).

6 **Tassilly, E.** and **Vincent, N.** A linear model for the corrugation of rails. *J. Sound Vibr.*, 1991, **150**(1), 25–45.

7 **Tassilly, E.** and **Vincent, N.** Rail corrugations: analytical models and field tests. *Wear*, 1991, **144**(1–2), 163–178.

8 **Elkins, J., Grassie, S.,** and **Handal, S.** Rail corrugation mitigation in transit, transit cooperative research program sponsored by the federal transit administration. *Res. Results Digest*, 1998, **26**, 1–33.

9 **Hempelmann, K.** *Short pitch corrugations on railway rails: a linear model for prediction*, 1994 (VDI Fortschritt-Berichte, VDI-Verlag, Dusseldorf).

10 **Hempelmann, K.** and **Knothe, K.** An extended linear model for the prediction of short pitch corrugation. *Wear*, 1996, **191**, 161–169.

11 **Gross-Thebing, A.** A lineare Modellierung des instationaren Rollkontaktes von Rad und Schiene. VDI Fortschritt-Berichte, Reihe 12, No. 199, Dusseldort, 1993.

12 **Müller, S.** A linear wheel-track model to predict instability and short pitch corrugation. *J. Sound Vibr.*, 1999, **227**, 899–913.

13 **Müller, S.** A linear wheel-rail model to investigate stability and corrugation on straight track. *Wear*, 2000, **243**, 122–132.

14 **Kalker, J. J.** *Three-dimensional elastic bodies in rolling contact*, 1990 (Kluwer, Dordrecht).

15 **Kalker, J. J.** A fast algorithm for the simplified theory of rolling contact. *Veh. Syst. Dyn.*, 1982, **11**, 1–13.

16 **Carter, F. W.** On the action of a locomotive driving wheel. *Proc. R. Soc., Lond., Ser. A*, 1926, **112**(760), 151–157.

17 **Barber, J. R.** *Elasticity*, 2nd edition, 2002 (Kluwer, Dordrecht).

18 **Grassie, S. L.** and **Edwards, J. W.** Development of corrugation as a result of varying normal load. In the 7th International Conference on Contact Mechanics and Wear of Rail/Wheel Systems (CM2006), Brisbane, Australia, 24–26 September 2006.

19 **Meehan, P. A., Daniel, W. J. T.,** and **Campey, T.** Prediction of the growth of weartype rail corrugation. *Wear*, 2005 **258**(7–8), 1001–1013.

20 **Nielsen, J. C. O., Ekberg, A.,** and **Lundén, R.** Influence of short-pitch wheel/rail corrugation on rolling contact fatigue of railway wheels. *Proc. IMechE, Part F: J. Rail and Rapid Transit*, 2005, **219**(3), 177–187.